PHOTOSYNTHETICA
International Journal for Photosynthesis Research

DOI 10.32615/ps.2023.008 PHOTOSYNTHETICA 61 (1): 97-107, 2023

# Downregulated expression of *TaDeg7* inhibits photosynthetic activity in bread wheat (*Triticum aestivum* L.)

F.F. LIU[*,**], G.P. LI[*,+], and H.W. LI[**,+]

*College of Life Sciences, Huaibei Normal University, 235000 Huaibei, China*[*]
*State Key Laboratory of Plant Cell and Chromosome Engineering, Institute of Genetics and Developmental Biology, Chinese Academy of Sciences, 100101 Beijing, China*[**]

## Abstract

Deg proteases play critical roles in photoprotection and PSII-repair circle, which remains elusive in cereal crops including wheat. Here, a Deg7-encoding gene *TaDeg7* was silenced in wheat *via* a *Barley stripe mosaic virus*-induced gene-silencing system (BSMV-VIGS). When the expression level of *TaDeg7* was downregulated, the photosynthetic activity including $CO_2$ assimilation rate, actual photochemical efficiency of PSII, and electron transport rate declined while the nonphotochemical quenching increased significantly. When grown in high light, the *BSMV:TaDeg7* plants accumulated more soluble sugar, malondialdehyde, and superoxide anion but had lower superoxide dismutase activity and less ascorbic acid. Additionally, the expression levels of *TaPsbA* and *TarbcS* were repressed in the *BSMV:TaDeg7* plants in high light. The *BSMV:TaDeg7* plants also were more sensitive to high-light stress. Collectively, it appeared that *TaDeg7* may be a potential target for wheat radiation-use efficiency improvement against high light stress.

*Keywords*: Deg7 protease; high light; photosynthetic efficiency; virus-induced gene silencing; wheat.

## Introduction

As a staple food crop, wheat contributes a significant food source for humans worldwide. Wheat yield should be increased continuously to meet the demand of the growing population. Identification of genes regulating photosynthetic activity is pivotal for wheat radiation-use efficiency (RUE) improvement and genetic yield

## Highlights

- Downregulated *TaDeg7* decreased the photosynthetic and photochemical efficiency of wheat
- Downregulated *TaDeg7* led to overaccumulation of ROS and enhanced photosensitivity to high light
- The regulation of expression levels of *TaDeg7* may be a potential target for wheat RUE improvement

*Received* 5 January 2023
*Accepted* 14 March 2023
*Published online* 30 March 2023

[+]Corresponding authors
e-mail: liguiping@chnu.edu.cn (G.P. Li)
hwli@genetics.ac.cn (H.W. Li)

*Abbreviations*: *ANOVA* – one-way analysis of variance; APX – ascorbate peroxidase; AsA – ascorbic acid; BSMV-VIGS – *Barley stripe mosaic virus*-induced gene silencing; Car – carotenoids; CAT – catalase; Chl *a*(*b*) – chlorophyll *a*(*b*); $C_i$ – intercellular $CO_2$ concentration; DHA – dehydroascorbate; $DI_0/RC$ – flux of energy dissipated in processes other than trapping per active PSII reaction center; dpi – days post inoculation; *E* – transpiration rate; $ET_0/RC$ – flux of electrons transferred from $Q_A^-$ to PQ per active PSII reaction center; ETR – electron transport rate; $F_v/F_m$ – maximum quantum yield of PSII photochemistry; $g_s$ – stomatal conductance; GSH – reduced glutathione; GSSG – oxidized glutathione; HL – high light; LL – low light; MDA – malondialdehyde; MV – methylviologen; NPQ – nonphotochemical quenching; $PI_{ABS}$ – performance index on absorption basis; $P_N$ – net photosynthetic rate; POD – peroxidase; PQ – plastoquinone; $PQH_2$ – plastoquinol; $Q_A^-$ – primary quinone electron acceptor of PSII; ROS – reactive oxygen species; RUE – radiation-use efficiency; SOD – superoxide dismutase; $\delta_{Ro}$ – final PSI acceptors; $\psi_{Eo}$ – efficiency with which a PSII trapped electron is transferred from $Q_A^-$ to PQ.

*Acknowledgments*: This work was supported by the Natural Science Foundation of China (No. 31872863) and the National Key Basic Research Program of China (No. 2015CB150106).

*Conflict of interest*: The authors declare that they have no conflict of interest.

improvement (Horton 2000). High light (HL) or other stressful conditions usually result in inhibition of photosynthesis, which is a constraint for achieving a high yield of cereal crops. Therefore, the regulation of photoinhibition is considered an approach for RUE improvement of cereal crops including wheat (Horton 2000). PSII is the main target of photoinhibition (Aro *et al.* 1993, Adir *et al.* 2003). The PSII-repair cycle, consisting of inactivation, degradation, and *de novo* synthesis of the D1 protein of the PSII reaction center, plays a pivotal role in photoprotection (Aro *et al.* 1993). Moreover, the overproduction of reactive oxygen species (ROS), such as superoxide anions ($O_2^{\bullet-}$), hydrogen peroxide ($H_2O_2$), singlet oxygen, *etc*., induced by HL or other stresses (drought, extreme temperature, and nutrition deficiency), causes oxidative damage and degradation of the D1 protein (Bradley *et al.* 1991, Miyao 1994). Photodamaged D1 protein is cooperatively cleaved by ATP-independent Deg proteases at both stromal and luminal sides of thylakoid membranes and ATP-dependent FtsH (Filamentation temperature-sensitive H) proteases at stroma (Kato *et al.* 2012). Deg proteases are periplasmic serine proteases that comprise an N-terminal protease domain with a His-Asp-Ser catalytic triad and a C-terminal PDZ domain(s) (Clausen *et al.* 2002). The PDZ domains regulate proteolytic activity and are necessary for the formation of functional oligomeric and protein–protein interactions (Huesgen *et al.* 2005). In *Arabidopsis*, sixteen Deg proteases have been identified, among which five (AtDeg1, AtDeg2, AtDeg5, AtDeg8, and AtDeg7) target chloroplasts, two (AtDeg10 and AtDeg14) locate in mitochondrion while one (AtDeg15) locates in peroxisome and one (AtDeg9) has nuclear localization (Schuhmann and Adamska 2012). The Deg proteases located in chloroplast play crucial roles in the degradation of the D1 protein (Schuhmann and Adamska 2012). However, the involvement of Deg2 in the degradation of the D1 protein is controversial (Haußühl *et al.* 2001, Huesgen *et al.* 2005).

Deg1, Deg5, and Deg8 are peripherally attached to the thylakoid lumen (Peltier *et al.* 2002, Schubert *et al.* 2002), whereas Deg2 and Deg7 are located in the thylakoid stroma (Haußühl *et al.* 2001, Sun *et al.* 2010). Downregulation of Deg1 (Kapri-Pardes *et al.* 2007), Deg5 and Deg8 (Sun *et al.* 2007a), and Deg7 (Sun *et al.* 2010) resulted in the accumulation of photodamaged D1 protein and enhanced photosensitivity of PSII to HL. Moreover, the downregulation of Deg1 leads to the inhibition of growth and reduction of leaf size and chlorophyll (Chl) content (Kapri-Pardes *et al.* 2007, Butenko *et al.* 2018). Although the growth rates of the mutants *deg5* and *deg8* (Sun *et al.* 2007a, Butenko *et al.* 2018) and *deg7* (Sun *et al.* 2010) are similar to the wild type under optimal conditions, they are more sensitive to stress, for instance, HL and high temperature, than the wild type (Sun *et al.* 2007b, Butenko *et al.* 2018). The *deg2* mutant not only enhanced photosensitivity to HL but also reduced leaf area (Luciński *et al.* 2011a), whereas the *deg5* mutant increased leaf area but reduced leaf thickness (Luciński *et al.* 2011b, Baranek *et al.* 2015). Deg7 protease, evolving from a whole-gene duplication/fusion of a Deg-like protease and twice as large as other Deg proteases, has two protease domains (one active and one degenerated) and four PDZ domains (Schuhmann *et al.* 2011). The *Arabidopsis deg7* mutant reduces PSII activity, enhances photosensitivity to HL, and grows slowly in HL (Sun *et al.* 2010).

Although Deg proteases had been well investigated in *Arabidopsis*, the roles of Deg proteases in cereal crops remain unclear. Several years ago, we initiated a project to explore the transcriptomic profiles of a new wheat line Xiaoyan 101 with improved RUE. The Deg7 encoding gene *TaDeg7* was found to be highly expressed in Xiaoyan101 compared to its parents (data not shown). In this study, *TaDeg7* was silenced in Xiaoyan 101 *via* the BSMV-VIGS method to explore its role in the regulation of photosynthetic activity and ROS homeostasis in wheat.

## Materials and methods

**Plant growth conditions**: An advanced winter wheat line *Triticum aestivum* cv. Xiaoyan 101, derived from a cross between two Chinese winter wheat varieties Xiaoyan 81 and Liangxing 99, was used in this study. Germinated seeds were cultivated in the nutrition medium and planted in a growth chamber as described previously (Li *et al.* 2017). The plants were first grown in LL at PPFD of 230 μmol $m^{-2}$ $s^{-1}$ in a growth chamber (*HP-1000GS*, *Wuhan Ruihua Instrument and Equipment Co. Ltd.*, Wuhan, China). For HL treatment, half of the plants grown in LL were transferred to HL (PPFD of 1,000 μmol $m^{-2}$ $s^{-1}$), supplied with the GE compact fluorescent light bulbs (*F55BX/840*, Boston, USA), in another growth chamber (*E36HO*, *Percival Scientific*, Iowa, USA) for 10 d. The growth conditions for LL and HL treatment were set at 20/15°C (day/night), 14-h photoperiod, and 40–60% of relative humidity.

**RNA isolation and first strand cDNA synthesis**: Total RNA was extracted from leaf samples with the *TRIzol* reagent (*Thermo Fisher Scientific*, Massachusetts, USA). RNA quantity and quality were determined with a spectrophotometer *Nanodrop 2000* (*Thermo Scientific*, Massachusetts, USA). First-strand cDNA was synthesized by using the *ReverTra Ace* qPCR RT *Master Mix* with gDNA Remover kit (*TOYOBO*, Osaka, Japan). The 10-μL reaction solution included 0.5 μg of total RNA, 2 μL of 4× *DN Master Mix*, 2 μL of 5× *RT Master Mix II*, and an appropriate amount of nuclease-free water. After incubation at 37°C for 15 min and 98°C for 5 min accordingly, the first-strand cDNA was diluted to a final volume of 50 μL.

**Construction of *γ:TaDeg7* vector**: The *γ:TaDeg7* vector was constructed according to Ying *et al.* (2020). A 169-bp cDNA fragment, homologous to *AtDeg7*, was isolated from Xiaoyan 101 with the gene-specific primers (forward: 5'-GCT AGC CCT GAG CGA AGA CAA GTA TTG-3' and reverse 5'-GCT AGC TTC CAT CTG

AAC CAA CCG-3'). The underlined sequences indicate the *Nhe* I restriction sites. The *TaDeg7* fragments were cloned with a *pGM-T Fast* kit (*Tiangen Biotech*, Beijing, China). Next, the target fragments were digested with *Nhe* I and inserted into the *Nhe* I digested γ vector with $T_4$ ligase, followed by transformation to the *E. coli* DH5α competent cells. Positive *γ:TaDeg7* clones were screened with the gene-specific primers and confirmed by sequencing.

***In vitro* BSMV RNAs transcription and BSMV-VIGS assay**: *In vitro* transcription of BSMV RNAs was conducted with a *RiboMAX™ Large Scale RNA Production System* kit (*Promega*, Wisconsin, USA) as described (Ying *et al*. 2020). After the plasmids of *α*, *γ:00*, and γ:*TaDeg7* were linearized with *Mlu* I and *β* plasmid was linearized with *Spe* I, the linearized plasmids were purified and used as templates for *in vitro* transcription. The 20-μL reaction solution consisted of 4 μL of $T_7$ transcription 5× buffer, 6 μL of rNTPs (25 mM ATP, CTP, UTP, and 3 mM GTP), 1.5 μL of 40 mM Ribo $m^7G$ Cap Analog, 2 μL of $T_7$ enzyme mix, 4 μL of linearized plasmids, and 2 μL of nuclease-free water and was incubated at 37°C for 2 h.

BSMV inoculation was performed according to Petty *et al*. (1989). An equal volume of RNAs *α*, *β*, and *γ:00* (or *γ:TaDeg7*) were mixed in 200 μL of GKP buffer, consisting of 50 mM glycine, 30 mM $K_2HPO_4$, 1% (w/v) bentonite, and 1% (w/v) celite at pH 9.2. Then, 10 μL of RNA mixture was pipetted and inoculated onto the second wheat leaves at 18 d after germination (three-leaf stage) with gloved index and thumb fingers. For simplicity, the RNA mixture of *α*, *β*, and *γ:00* (empty vector as control) inoculated plants was named *BSMV:γ00* while the *α*, *β*, and *γ:TaDeg7* RNA mixture-inoculated plants were named as *BSMV:TaDeg7*.

**Gene expression analysis**: The qPCR analysis was performed on the *StepOnePlus™* Real-Time PCR Systems (*Thermo Fisher Scientific*, Massachusetts, USA). The 10 μL of reaction solution included 2 μL of diluted cDNA, 5 μL of 2× *PowerUp SYBR Green Master Mix* (*Thermo Fisher Scientific*, USA), 0.2 μL of each of forward and reverse gene-specific primers and 2.6 μL of $H_2O$. The primers for *TaDeg7* (forward 5'-ACC GAC GAG CAA GGG AGA GT-3' and reverse 5'-CCA AAG AGC TGG CTG GAA AT-3') and *TaPsbA* (forward 5'-TTA TAT GGG TCG TGA GTG GGA ACT-3' and reverse 5'-ATA TGC AAC AGC AAT CCA AGG A-3') were designed according to TraesCS6B02G170600 and NC_002762.1, respectively. The primers for *TarbcS* have been previously described by Li *et al*. (2019) and Ying *et al*. (2020). According to Uauy *et al*. (2006), the *TaActin* was taken as an internal reference gene. Relative expression of the investigated genes was calculated following the $2^{-\Delta\Delta}C_T$ method (Schmittgen and Livak 2008). Three independent biological repeats and four technique repeats were carried out for each biological repeat.

**Gas-exchange measurement** was conducted in the morning at 9:00–11:00 h on the middle parts of the fully expanded sixth leaves at 33 dpi. The net photosynthetic rate ($P_N$), stomatal conductance ($g_s$), intercellular $CO_2$ concentration ($C_i$), and transpiration rate ($E$) were output from a portable leaf gas-exchange system *GFS-3000* (*Walz*, Effeltrich, Germany). When measuring, the light intensity, $CO_2$ concentration, relative humidity, temperature, and airflow rate were set to PPFD of 800 μmol $m^{-2}$ $s^{-1}$, 400 μmol $mol^{-1}$, 60%, 27°C, and 750 μmol $s^{-1}$, respectively. After light induction for 15 min, the gas-exchange parameters were recorded and output directly from the software *GFS-Win* (*version 3.70*). For each genotype, 6–8 plants were measured, and each plant was recorded twice. Three independent measurements were conducted.

**Chl *a* fluorescence** was measured with an *IMAGING-PAM M-Series* Chlorophyll Fluorescence System (*MAXI version*, *Walz*, Effeltrich, Germany). After dark adaptation for 30 min, the middle parts of the fully expanded sixth leaves were measured at 30 dpi. The actinic light intensity was set as 500 μmol(photon) $m^{-2}$ $s^{-1}$, the other parameters were set as default. After measuring for 602 s (light duration was 560 s), the nonphotochemical quenching (NPQ), $\Phi_{PSII}$, and ETR were output from the software *ImagingWin* (*version 2.41a*, *Walz*, Effeltrich, Germany). In addition, the light-response curve was conducted following the default parameters by using the *IMAGING-PAM M-Series* Chlorophyll Fluorescence System. The active light intensity was set as PPFD of 0, 25, 100, 300, 350, 400, 500, 600, 800; 1,000; 1,200; 1,400; 1,600; 1,800; and 2,000 μmol $m^{-2}$ $s^{-1}$, respectively.

In addition, fast transient Chl *a* fluorescence was measured with a *Handy-PEA* fluorescence meter (*Hansatech*, Norfolk, UK) after dark adaptation for 30 min. The saturated flash light intensity was 3,000 μmol(photon) $m^{-2}$ $s^{-1}$ and the light duration was 1 s. The maximum quantum yield of PSII photochemistry ($F_v/F_m$) and JIP-test fluorescence parameters including $PI_{ABS}$, $\psi_{Eo}$, $\delta_{Ro}$, $ET_0$/RC, and $DI_0$/RC were output from the software *PEA Plus* (*version 1.10*). These JIP-test parameters were computed as described by Stirbet *et al*. (2018).

**Biochemical and physiological assay of photosynthetic constitutes**: At 22 dpi, the fourth leaves were sampled for biochemical and physiological assay. Rubisco was extracted and assayed for activity with a Rubisco kit (*Comin*, Suzhou, China) following Wu *et al*. (2018). The absorbance at 340 nm was recorded with a *Multiskan MK3 Spectrum* spectrophotometer (*Thermo Scientific*, Massachusetts, USA). One unit of Rubisco activity was defined as the amount of enzyme to oxidize 1 nmol(NADH) per min at 25°C. Photosynthetic pigments were extracted in 80% acetone and the content of Chl (*a*+*b*), Chl *a*, Chl *b*, and Car was determined according to Arnon (1949).

**Assay of the ROS production and removal system**: The MDA and soluble sugar were extracted and quantified according to Ledwożyw *et al*. (1986). The content of $O_2^{\bullet-}$ was measured with an oxygen-free radical kit (*Comin*, Suzhou, China) described by Elstner and Heupel (1976).

$NH_2OH$ was used as a spectrophotometric probe for $O_2^{\bullet-}$. The content of $H_2O_2$ was measured following Junglee *et al*. (2014), which is based on potassium iodide oxidation by $H_2O_2$. The activity of superoxide dismutase (SOD, EC 1.15.1.1), catalase (CAT, EC 1.11.1.6), ascorbate peroxidase (APX, EC 1.11.1.11), and peroxidase (POD, EC 1.11.1.7) was evaluated with the corresponding kits (*Comin*, Suzhou, China) following the manufacturer's instructions (Chen *et al*. 2017, Su *et al*. 2018, Pan *et al*. 2019). One unit of the SOD activity was defined as the amount of enzyme to inhibit nitroblue tetrazolium photoreduction by 50% (Peskin and Winterbourn 2000). One unit of the CAT activity was defined as the amount of enzyme to reduce 1 nmol($H_2O_2$) per min (Sima *et al*. 2011). One unit of the APX was defined as the amount of enzyme to oxidize 1 μmol(AsA) per min (Ullah *et al*. 2016). One unit of the POD activity was defined as the amount of enzyme to increase 0.005 of the absorbance at 470 nm wavelength per min (Wang *et al*. 2014). The AsA and DHA were extracted and quantified according to Stevens *et al.* (2006). About 0.05 g of leaf samples were homogenized and extracted in 1 mL of 6% (w/v) tricarboxylic acid cycle (TCA), followed by centrifugation at 13,000 × *g* for 5 min at 4°C. The supernatant was collected to determine the content of AsA and DHA. GSH and GSSG were extracted and quantified with the GSH and GSSG kits (*Comin*, Suzhou, China) as described by Su *et al*. (2018).

**Short-term HL treatment**: Detached leaf segments, 2–3 cm long, were exposed to HL in the presence or absence of methyl viologen (MV). Before HL treatment, the leaf segments were immersed in 20 μmol $L^{-1}$ MV for 1.5 h in darkness at room temperature. Meanwhile, deionized water was used as a control. Then, the leaf segments were immersed in water and exposed to 1,300 μmol(photon) $m^{-2}$ $s^{-1}$ for 1 h.

**Data analysis**: Data were represented as mean ± SE (standard error). One-way analysis of variance (*ANOVA*) and multiple comparative analyses were performed with *IBM SPSS Statistics* (*version 19.0*). Multiple comparisons of means were performed using the least significant difference (LSD) *t*-test at $P$=0.05. Figures were depicted with the software *SigmaPlot* (*version 12.0*).

## Results

**Photosynthetic activity**: A 169-bp cDNA fragment, with the highest sequence identity (97–100%) to Chinese Spring Deg7 protease encoding genes (IWGSCv1.0: TraesCS6D01G162300LC.1, TraesCS6B01G170600.1, and TraesCS6A01G129000LC.1), was used to construct the *BSMV:TaDeg7* vector. The deduced amino acid sequence for this cDNA fragment was homologous to the PDZ domain of *Arabidopsis* DEG7 protein (AT3G03380.1). Meanwhile, the empty vector *BSMV:γ00* for mock infection was taken as control. As shown in Fig. 1*A*, the leaves of both the *BSMV:TaDeg7* and *BSMV:γ00* plants exhibited typical BSMV infection stripe necrosis. The transcripts of *TaDeg7* declined drastically in the *BSMV:TaDeg7* plants compared to the *BSMV:γ00* plants (Fig. 1*B*), indicating that *TaDeg7* was successfully downregulated. Net photosynthetic rate ($P_N$), stomatal conductance ($g_s$), intercellular $CO_2$ concentration ($C_i$), and transpiration rate ($E$) in the *BSMV:TaDeg7* plants all declined significantly in comparison to those in the *BSMV:γ 00* plants (Fig. 1*C–F*). Chl *a* fluorescence slow kinetics demonstrated that the actual photochemical efficiency of PSII ($\Phi_{PSII}$, Fig. 1*G*) and electron transport rate (ETR, Fig. 1*I*) declined while the NPQ was enhanced significantly in the *BSMV:TaDeg7* plants (Fig. 1*H*). However, no significant difference was observed for the fresh mass, tiller number, root length, and plant height between the *BSMV:TaDeg7* and the control plants whether grown in low light (LL) or HL (Fig. 1S, *supplement*). It appeared that the silencing of *TaDeg7* reduced the $CO_2$ assimilation rate and PSII photochemical activity.

**Photochemical efficiency in both LL and HL**: To investigate the effects of silencing of *TaDeg7* on PSII photochemical efficiency, both the *BSMV:TaDeg7* and *BSMV: 00* plants were grown in LL and HL for 10 d after 12 d post inoculation (dpi). The Chl *a* fluorescence parameters including $F_v/F_m$, performance index on absorption basis ($PI_{ABS}$), efficiency with which a PSII trapped electron is transferred from $Q_A^-$ to PQ ($\psi_{Eo}$), efficiency with which an electron from $PQH_2$ is transferred to final PSI acceptors ($\delta_{Ro}$), a flux of electrons transferred from $Q_A^-$ to PQ per active PSII reaction center ($ET_0$/RC), and flux of energy dissipated in processes other than trapping per active PSII reaction center ($DI_0$/RC) were determined in the fourth leaves of both the BSMV-infected plants at 22 dpi. For both genotypes, under HL conditions, the $F_v/F_m$, $PI_{ABS}$, $\psi_{Eo}$, and $ET_0$/RC were reduced by nearly 10, 60, 20, and 10% than those under LL conditions, respectively. However, HL enhanced the $\delta_{Ro}$ and $DI_0$/RC for both genotypes by more than 20 and 40% relative to LL (Fig. 2). The $F_v/F_m$, $PI_{ABS}$, $\psi_{Eo}$, and $ET_0$/RC were lower in the *BSMV:TaDeg7* plants than those in the *BSMV:γ 00* plants whether grown in LL or HL. However, the $\delta_{Ro}$ and $DI_0$/RC were at least 10% higher in the *BSMV:TaDeg7* plants than those in the control plants in HL although no significant differences were observed in LL.

**The content of photosynthetic pigments**: To explore the influence of silencing of *TaDeg7* on the content of photosynthetic pigments, the content of Chl (*a*+*b*), Chl *a*, Chl *b*, and carotenoids (Car) were assayed in the fourth leaves of both the *BSMV:TaDeg7* and *BSMV:γ 00* plants at 25 dpi. As shown in Fig. 3, relative to LL, HL reduced the Chl content (Fig. 3*A–C*) and the ratio of Chl (*a*+*b*)/Car to approximately 95 and 50% (Fig. 3*F*), respectively, but enhanced the Car content (Fig. 3*D*) and the ratio of Chl *a*/*b* (Fig. 3*E*) over 20 and 30% in both the BSMV-infected plants. In LL, the Chl (*a*+*b*) (Fig. 3*A*), Chl *a* (Fig. 3*B*), Chl *b* (Fig. 3*C*), and Chl (*a*+*b*)/Car (Fig. 3*F*) were significantly higher but the Chl *a*/*b* (Fig. 3*E*) was lower in the *BSMV:TaDeg7* plants than those in the *BSMV:γ 00* plants. However, in HL only the Car content

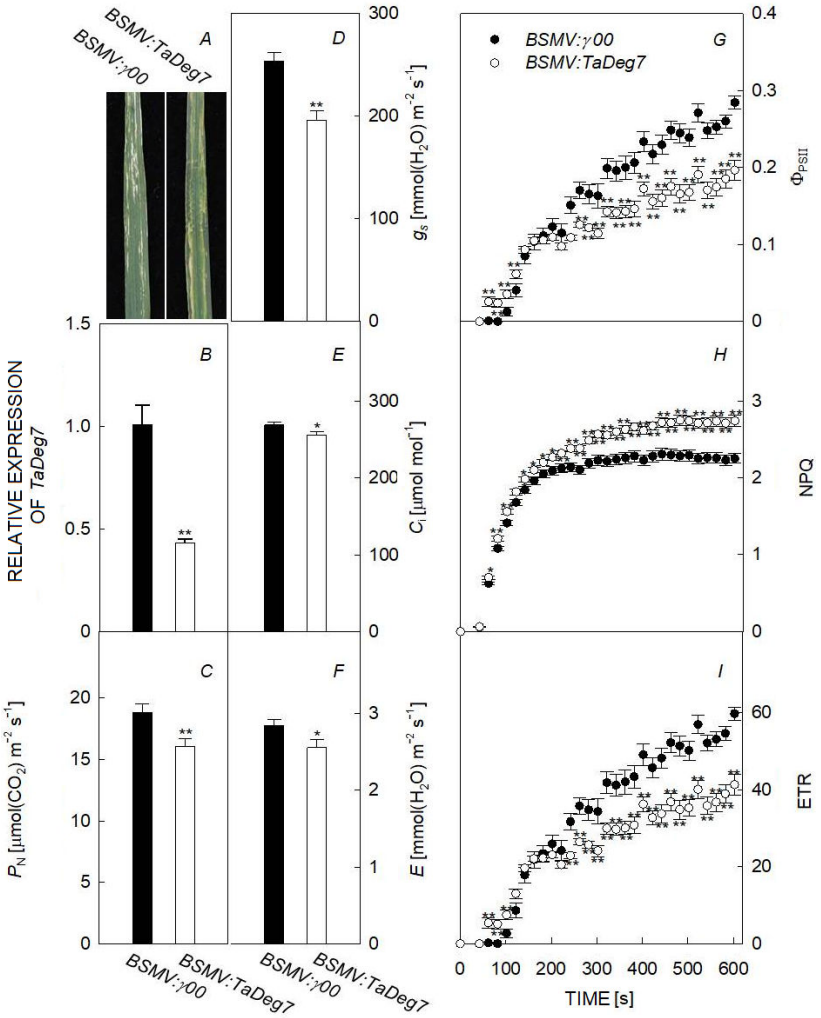


Fig. 1. Infection phenotypes, expression of *TaDeg7*, gas exchange, and Chl *a* fluorescence kinetic curves in the *BSMV:TaDeg7* and *BSMV:γ 00* plants. (*A*) A photograph of the *BSMV:γ 00* and *BSMV:TaDeg7* infected leaves; (*B*) relative expression of *TaDeg7*; (*C*) net photosynthetic rate ($P_N$); (*D*) stomatal conductance ($g_s$); (*E*) intercellular $CO_2$ concentration ($C_i$); (*F*) transpiration rate ($E$); (*G*) actual photochemical efficiency of PSII ($\Phi_{PSII}$); (*H*) nonphotochemical efficiency (NPQ); (*I*) electron transport rate (ETR). Data are represented as mean ± SE. * and ** denoted significant difference at $p<0.05$ and $p<0.01$, respectively.

differed significantly between the two genotypes, which was reduced in the *TaDeg7* silencing plants.

**The expression levels of *TaPsaA* and *TarbcS* and Rubisco activity**: The expression levels of the D1 protein of PSII reaction center encoding gene *TaPsbA* and the small subunit of Rubisco encoding gene *TarbcS* as well as the Rubisco activity was assayed in both the *BSMV:TaDeg7* and *BSMV:γ 00* plants grown in LL and HL at 25 dpi. The mRNA transcripts of *TaPsbA* were significantly lower in the *BSMV:TaDeg7* plants than those in the control plants whether in LL or HL (Fig. 4*A*). However, the expression levels of *TarbcS* were significantly higher in LL but lower in HL in the *BSMV:TaDeg7* plants compared to that in the *BSMV:γ 00* plants (Fig. 4*B*). Consistently, the Rubisco activity was significantly higher in the *BSMV:TaDeg7* plants than that in the control plants in LL. However, no significant difference in the Rubisco activity was observed between the BSMV-infected plants in HL (Fig. 4*C*).

**Overproduction of ROS**: The content of soluble sugar, malondialdehyde (MDA), $O_2^{\bullet-}$, $H_2O_2$, and antioxidants as well as the activity of ROS-removing enzymes were determined in the fourth leaves of both the *BSMV:TaDeg7* and *BSMV:γ 00* plants. As shown in Table 1, in LL, the content of $H_2O_2$, ascorbic acid (AsA), reduced glutathione (GSH), and oxidized glutathione (GSSG) were significantly higher but the ascorbate peroxidase (APX) activity was lower in the *BSMV:TaDeg7* plants compared to those in the control plants. However, in HL, no significant differences were observed in the content of $H_2O_2$ and GSH between the two BSMV-infected plants. On the contrary, the content of AsA and GSSG decreased while the APX activity was elevated in the *BSMV:TaDeg7* plants in comparison to those in the *BSMV:γ 00* plants in HL. In addition, the *BSMV:TaDeg7* plants accumulated more soluble sugar, MDA, and $O_2^{\bullet-}$ but had lower activity of superoxide dismutase (SOD) and peroxidase (POD) in HL. Also, in comparison with the *BSMV:γ 00* plants, the *BSMV:TaDeg7* plants possessed a higher ratio of GSH/GSSG but a lower ratio of AsA/dehydroascorbate (DHA) in HL. However, no significant difference was observed for the catalase (CAT) activity and DHA content between the *BSMV:TaDeg7* and *BSMV:γ 00* plants whether grown in LL or HL, indicating that they were less influenced

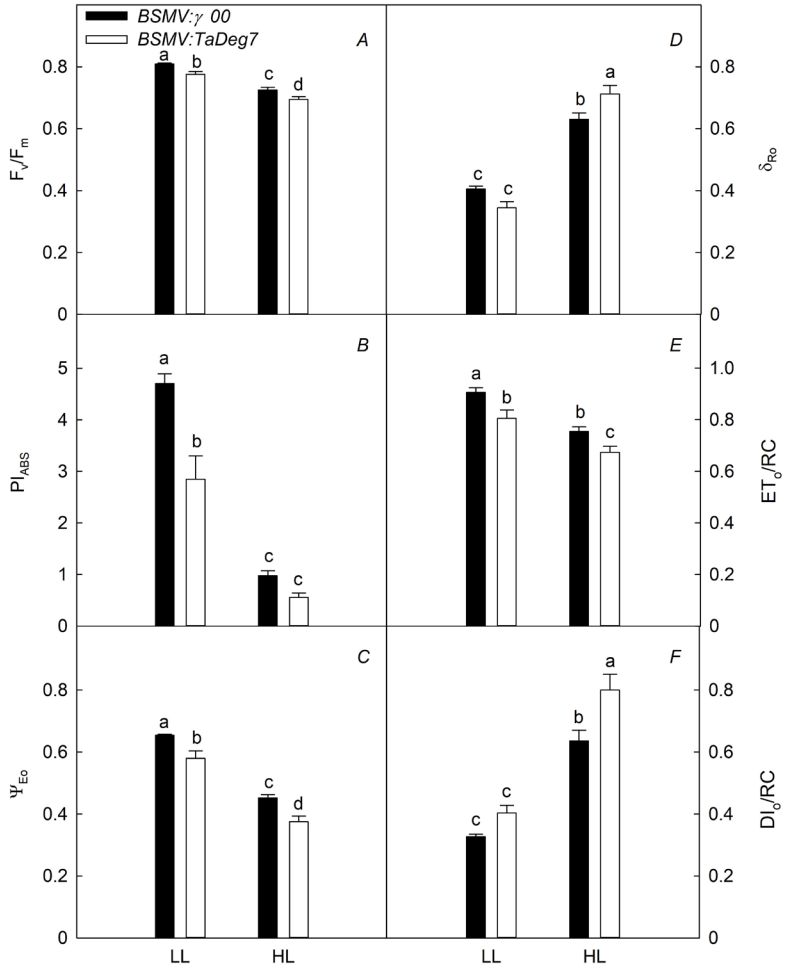


Fig. 2. Chl *a* fluorescence in the *BSMV:TaDeg7* and *BSMV:γ 00* plants grown in LL and HL. (*A*) The maximum quantum yield of PSII photochemistry ($F_v/F_m$); (*B*) performance index on absorption basis ($PI_{ABS}$); (*C*) efficiency with which a photosystem II (PSII) trapped electron is transferred from $Q_A^-$ to PQ ($\psi_{Eo}$); (*D*) efficiency with which an electron from $PQH_2$ is transferred to final PSI acceptors ($\delta_{Ro}$); (*E*) the flux of electrons transferred from $Q_A^-$ to PQ per active PSII ($ET_0/RC$); (*F*) the flux of energy dissipated in processes other than trapping per active PSII ($DI_0/RC$). Data are represented as mean ± SE. *Different letters* indicate the significant difference at $p<0.05$.

when *TaDeg7* was silenced. Collectively, when *TaDeg7* was silenced, the wheat plants accumulated more $H_2O_2$ in LL and more $O_2^{\bullet-}$ in HL, indicative of overproduction of ROS in the *BSMV:TaDeg7* plants. Particularly in HL, the overproduction of ROS seemed to result from the inhibition of the SOD activity.

**Downregulation of *TaDeg7* enhanced photosensitivity to HL**: Light-response curve of Chl *a* fluorescence showed that the $\Phi_{PSII}$ and ETR were lower while the NPQ was higher in the *BSMV:TaDeg7* plants in comparison with the control plants (Fig. 5), which was consistent with the kinetic curves (Fig. 1*G–I*). The $\Phi_{PSII}$ decreased while the NPQ increased consistently with the enhancement of light intensity. The ETR increased with the rise of light intensity below PPFD of 1,500 μmol $m^{-2}$ $s^{-1}$; however, it declined when the PPFD was over than that. The difference in ETR between the *BSMV:TaDeg7* and *BSMV:γ 00* plants increased when the PPFD was over 800 μmol $m^{-2}$ $s^{-1}$, demonstrating that the *BSMV:TaDeg7* plants were more sensitive to HL. In addition, the $F_v/F_m$ was significantly lower in the *BSMV:TaDeg7* plants when exposed to HL in the presence of MV (Fig. 6), suggesting that silencing of *TaDeg7* enhanced wheat photosensitivity to photooxidative stress.

## Discussion

HL-induced photooxidative stress is a significant constraint for wheat yield formation. During the grain-filling stage, it usually leads to premature leaf senescence and grain yield loss (Li *et al*. 2010, 2017; Liu *et al*. 2019). Therefore, identifying genes regulating photoinhibition will provide potential targets for wheat RUE and genetic yield improvement (Ying *et al*. 2020). Although the roles of Deg proteases in the regulation of photoinhibition have been well studied in *Arabidopsis*, they remain elusive in cereal crops such as wheat. Deg proteases encoding genes, such as *Deg1*, *Deg2*, and *Deg8*, can be induced by HL (Sinvany-Villalobo *et al*. 2004). The *Arabidopsis deg* mutants enhanced photosensitivity to HL (Sun *et al*. 2007a, 2010; Butenko *et al*. 2018). Our transcriptomic data showed that *TaDeg7* is highly expressed in Xiaoyan 101 with tolerance to HL relative to its parents. Further quantitative polymerase chain reaction (qPCR) confirmed that the expression levels of *TaDeg7* differed significantly among many Chinese winter wheat varieties (data not shown). The primary study indicated that wheat varieties highly expressing *TaDeg7* such as Xiaoyan 101 were more tolerant to HL (data not shown). Hence, it seems that the expression levels of *TaDeg7* may play a role in

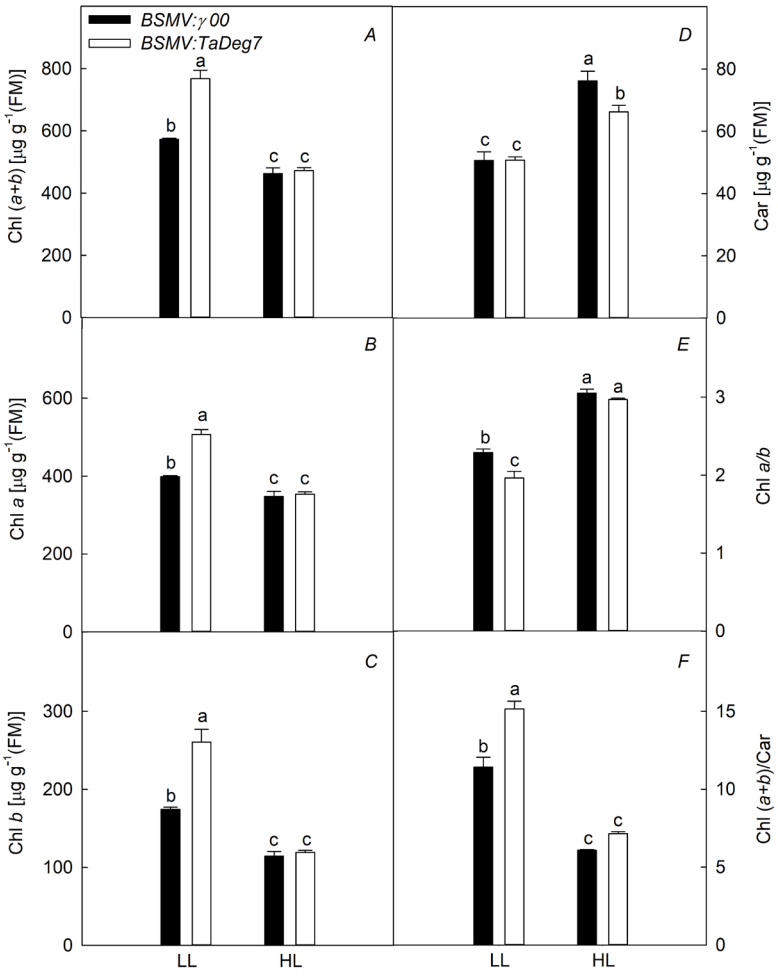


Fig. 3. The content of photosynthetic pigments in the *BSMV:TaDeg7* and *BSMV:γ 00* plants grown in LL and HL. (*A*) Total chlorophyll [Chl (*a*+*b*)] content; (*B*) Chl *a* content; (*C*) Chl *b* content; (*D*) carotenoids (Car) content; (*E*) ratios of Chl *a*/*b*; (*F*) ratios of Chl (*a*+*b*)/Car. Data are represented as mean ± SE. *Different letters* indicate the significant difference at $p<0.05$.

the regulation of photosynthetic activity.

BSMV-VIGS is an efficient tool for the study of gene functions in monocot plants including barley and wheat (Holzberg *et al.* 2002, Hein *et al.* 2005, Scofield *et al.* 2005, Chen *et al.* 2015, Ying *et al.* 2020). When the transcripts of *TaDeg7* were reduced to 42.9% in Xiaoyan 101 *via* BSMV-VIGS, both the photosynthetic rate and photochemical efficiency of PSII declined markedly. The reduction of the $CO_2$ assimilation rate appeared to be ascribed to stomatal limitation and the decline of the photochemical efficiency of PSII. Chl *a* fluorescence slow kinetic and light-response curves demonstrated that NPQ elevated in the *BSMV:TaDeg7* plants. Additionally, Chl *a* fluorescence JIP-test also confirmed the enhancement of thermal energy dissipation ($DI_0$/RC) in the *BSMV:TaDeg7* plants, especially in HL. In addition, the efficiency with which an electron from $PQH_2$ is transferred to final PSI acceptors ($\delta_{Ro}$) elevated considerably in the *BSMV:TaDeg7* plants in HL. Collectively, silencing of *TaDeg7* promoted photoinhibition of PSII and subsequently reduced the $CO_2$ assimilation rate in wheat. Reversible photoinhibition acts as a photoprotection mechanism against the overproduction of ROS and photodamage in PSI (Tikkanen *et al.* 2014). Taken together, more light energy was dissipated as heat while less energy was absorbed and transferred to PSII for $CO_2$ assimilation when the expression levels of *TaDeg7* were downregulated in wheat, especially in HL.

In this study, silencing of *TaDeg7* was also found to influence the content of photosynthetic pigments. For instance, in LL the content of Chl (*a*+*b*), Chl *a*, and Chl *b* was significantly higher in the *BSMV:TaDeg7* plants than those in the control plants. But the Chl *a*/*b* was lower in the *BSMV:TaDeg7* plants in LL. However, in HL, no significant difference was found in Chl content between the *BSMV:TaDeg7* and *BSMV:γ 00* plants. The Car content was significantly lower in the *BSMV:TaDeg7* plants in HL though no significant difference was found for it in LL between the two BSMV-infected plants. As Car plays a photoprotective role by quenching the triplet Chl and scavenging ROS (Choudhury and Behera 2001), the reduction of the Car indicated that the photoprotection role of the Car was suppressed in the *BSMV:TaDeg7* plants in HL. In addition, the expression levels of *TarbcS* as well as the Rubisco activity were higher in the *BSMV:TaDeg7* plants in LL. However, in HL the expression levels of *TarbcS* declined markedly in the *BSMV:TaDeg7* plants though the Rubisco activity changed little. Taken together, the *BSMV:TaDeg7* plants had higher Chl content and

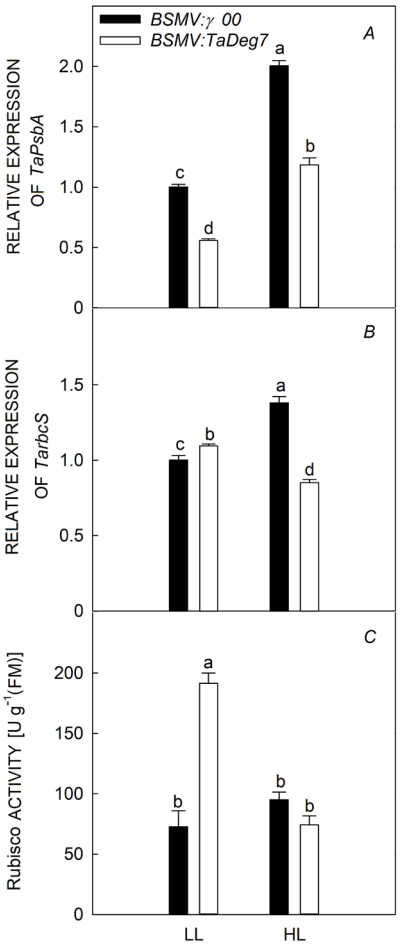


Fig. 4. Expression of *TaPsbA* (*A*) and *TarbcS* (*B*) and Rubisco activity (*C*) in the *BSMV:TaDeg7* and *BSMV:γ 00* plants grown in LL and HL. Data are represented as mean ± SE. *Different letters* indicate the significant difference at $p<0.05$.

Rubisco activity in LL but possessed lower expression levels of *TarbcS* and content of the Car in HL.

Several lines of evidence demonstrate that the Deg proteases cleave not only the D1 protein but also other proteins. For instance, an *in vitro* assay showed that recombinant Deg1 can degrade PsbO and plastocyanin, suggesting that PsbO and plastocyanin may be Deg-protease substrates (Chassin *et al*. 2002). In addition, *in vitro* digestion of isolated *Arabidopsis thaliana* thylakoids demonstrated that Deg7 protease has proteolytic activity on PSII proteins including D1, D2, CP43, and CP47 (Sun *et al*. 2010). In this study, the expression of the D1 protein-encoding gene *TaPsbA* was repressed in the *BSMV:TaDeg7* plants in both LL and HL. The suppression of *TaPsbA* in the *BSMV:TaDeg7* plants may be ascribed to the feedback inhibition of the accumulated damaged D1 protein (Sun *et al*. 2010). A further comparison should be performed to determine the number of photosynthetic proteins including D1 in the *BSMV:TaDeg7* plants.

The photoinhibition process usually promotes the overproduction of ROS which ultimately results in lipid membrane peroxidation (Bradley *et al*. 1991, Miyao 1994). The *BSMV:TaDeg7* plants accumulated more $H_2O_2$ in LL and more $O_2^{\bullet-}$ in HL in comparison to the *BSMV:γ 00* plants, indicating that silencing of *TaDeg7* promoted overproduction of ROS. In HL, ROS accumulation led to the overproduction of MDA in the *BSMV:TaDeg7* plants. As MDA can bring about secondary oxidative damage to proteins (Traverso *et al*. 2004), higher accumulation of MDA indicated that severe lipid peroxidation occurred in the *BSMV:TaDeg7* plants. Lipid peroxidation products can in turn result in oxidative modification of PSII proteins (Pospíšil and Yamamoto 2017) and thus deteriorate the photoinhibition process. A previous study revealed that the *deg5* mutants accumulate more starch than the wild type (Baranek *et al*. 2015). In this study, the *BSMV:TaDeg7* plants generated more soluble sugar

Table 1. Comparison of reactive oxygen species (ROS) homeostasis in the *BSMV:γ 00 and BSMV:TaDeg7* plants grown in LL and HL. Data are presented as mean ± SE. The different *superscript letters* denote significant differences at $p<0.05$.

| Traits | LL | | HL | |
|---|---|---|---|---|
| | *BSMV:γ00* | *BSMV:TaDeg7* | *BSMV:γ00* | *BSMV:TaDeg7* |
| Soluble sugar content [μmol $g^{-1}$(FM)] | $103.8 \pm 2.5^{c}$ | $107.2 \pm 4.6^{c}$ | $130.8 \pm 5.5^{b}$ | $196.6 \pm 7.8^{a}$ |
| MDA content [nmol $g^{-1}$(FM)] | $29.28 \pm 0.6^{c}$ | $27.16 \pm 1.54^{c}$ | $41.34 \pm 0.91^{b}$ | $49.07 \pm 2.23^{a}$ |
| $O_2^{\bullet-}$ content [nmol $g^{-1}$(FM)] | $133.9 \pm 12.0^{c}$ | $111.7 \pm 8.9^{c}$ | $282.7 \pm 22.0^{b}$ | $519.6 \pm 43.7^{a}$ |
| $H_2O_2$ content [μmol $g^{-1}$(FM)] | $2.02 \pm 0.04^{c}$ | $2.50 \pm 0.11^{b}$ | $5.91 \pm 0.10^{a}$ | $5.67 \pm 0.08^{a}$ |
| SOD activity [KU $g^{-1}$(FM)] | $1.08 \pm 0.22^{b}$ | $0.96 \pm 0.05^{b}$ | $1.60 \pm 0.02^{a}$ | $1.04 \pm 0.07^{b}$ |
| CAT activity [KU $g^{-1}$(FM)] | $2.88 \pm 0.39^{b}$ | $3.11 \pm 0.23^{ab}$ | $3.42 \pm 0.12^{ab}$ | $3.50 \pm 0.13^{a}$ |
| APX activity [U $g^{-1}$(FM)] | $6.11 \pm 0.32^{a}$ | $3.67 \pm 0.50^{b}$ | $4.33 \pm 0.27^{b}$ | $5.46 \pm 0.19^{a}$ |
| POD activity [KU $g^{-1}$(FM)] | $589.1 \pm 39.8^{b}$ | $555.3 \pm 48.0^{b}$ | $826.5 \pm 18.8^{a}$ | $621.5 \pm 41.9^{b}$ |
| ASA content [μmol $g^{-1}$(FM)] | $0.21 \pm 0.02^{d}$ | $0.27 \pm 0.01^{c}$ | $0.65 \pm 0.01^{a}$ | $0.55 \pm 0.02^{b}$ |
| DHA content [μmol $g^{-1}$(FM)] | $0.94 \pm 0.03^{a}$ | $1.02 \pm 0.01^{a}$ | $1.00 \pm 0.04^{a}$ | $1.03 \pm 0.02^{a}$ |
| ASA/DHA | $0.23 \pm 0.02^{c}$ | $0.26 \pm 0.02^{c}$ | $0.66 \pm 0.03^{a}$ | $0.54 \pm 0.02^{b}$ |
| GSH content [μmol $g^{-1}$(FM)] | $0.73 \pm 0.02^{c}$ | $0.99 \pm 0.06^{b}$ | $1.66 \pm 0.01^{a}$ | $1.73 \pm 0.07^{a}$ |
| GSSG content [μmol $g^{-1}$(FM)] | $0.18 \pm 0.01^{c}$ | $0.21 \pm 0.01^{ab}$ | $0.23 \pm 0.01^{a}$ | $0.19 \pm 0.01^{bc}$ |
| GSH/GSSG | $4.07 \pm 0.16^{c}$ | $4.71 \pm 0.37^{c}$ | $7.23 \pm 0.24^{b}$ | $9.27 \pm 1.07^{a}$ |

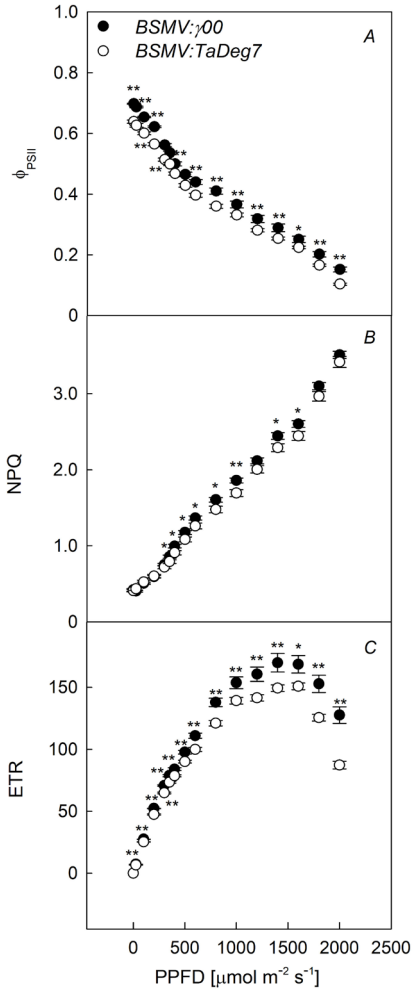


Fig. 5. Light-response curves of the actual photochemical efficiency of PSII ($\Phi_{PSII}$) (*A*), nonphotochemical quenching (NPQ) (*B*), and electron transport rate (ETR) (*C*) in the *BSMV:TaDeg7* and *BSMV:γ 00* plants. Data are represented as mean ± SE. * and ** denoted significant difference at $p<0.05$ and $p<0.01$, respectively.

than the control plants in HL. Sulmon *et al*. (2004) reported that sucrose treatment decreased *psbA* mRNA and D1 protein levels in *Arabidopsis*. Sugar was considered to be involved in ROS balance and response to oxidative stress in plants (Couée *et al*. 2006). Hence, it seemed that high soluble sugar content was associated with ROS accumulation and suppression of *TaPsbA* in the *BSMV:TaDeg7* plants grown in HL. The ROS accumulation in the *BSMV:TaDeg7* plants can be ascribed to the reduction of APX activity in LL and SOD activity in HL, respectively. In addition, a decline of AsA and AsA/DHA may be also associated with a high accumulation of ROS in the *BSMV:TaDeg7* plants in HL. Taken together, silencing of *TaDeg7* ultimately led to a reduction of the AsA content and SOD activity and accumulation of the contents of sugar, MDA, and $O_2^{\bullet-}$ in HL.

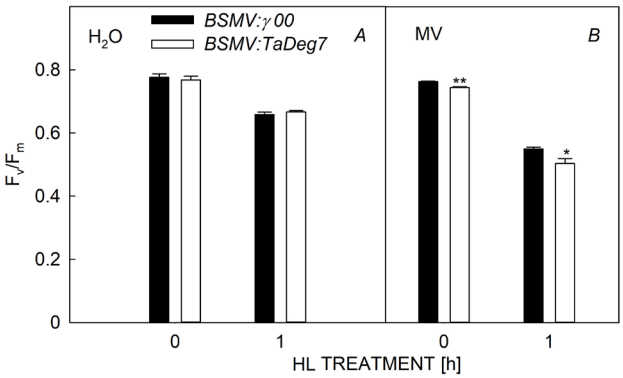


Fig. 6. The maximum quantum yield of PSII photochemistry ($F_v/F_m$) in the *BSMV:TaDeg7* and *BSMV:γ 00* plants subjected to HL treatment in the absence (*A*) and presence of 20 μmol $L^{-1}$ methylviologen (MV) (*B*). Data are represented as mean ± SE. * and ** denoted significant difference at $p<0.05$ and $p<0.01$, respectively.

**Conclusion**: Downregulation of *TaDeg7* in wheat *via* BSMV-VIGS resulted in a reduction of $CO_2$ assimilation and photochemical efficiency but enhancement of NPQ and energy dissipation. The expression levels of *TaPsbA* declined in the *BSMV:TaDeg7* plants compared with the *BSMV:γ 00* plants. Although the *BSMV:TaDeg7* plants had higher Chl content, Rubisco activity, and expression levels of *TarbcS* in LL, they accumulated more soluble sugar, MDA, and $O_2^{\bullet-}$ but inhibited *TarbcS* and declined SOD activity and AsA content in HL. In addition, photosensitivity to HL was enhanced in the *BSMV:TaDeg7* plants. Taken together, it appeared that the expression of *TaDeg7* plays a role in the regulation of photosynthetic activity, particularly in HL. Therefore, the regulation of expression levels of *TaDeg7* may be a potential target for wheat RUE improvement. Molecular markers associated with high expression of *TaDeg7* can be developed in the future.

## References

Adir N., Zer H., Shochat S., Ohad I.: Photoinhibition – a historical perspective. – Photosynth. Res. **76**: 343-370, 2003.

Arnon D.I.: Copper enzymes in isolated chloroplasts. Polyphenoloxidase in *Beta vulgaris*. – Plant Physiol. **24**: 1-15, 1949.

Aro E.-M., Virgin I., Andersson B.: Photoinhibition of photosystem II. Inactivation, protein damage and turnover. – BBA-Bioenergetics **1143**: 113-134,1993.

Baranek M., Wyka T.P., Jackowski G.: Downregulation of chloroplast protease AtDeg5 leads to changes in chronological progression of ontogenetic stages, leaf morphology and chloroplast ultrastructure in *Arabidopsis*. – Acta Soc. Bot. Pol. **84**: 59-70, 2015.

Bradley R.L., Long K.M., Frasch W.D.: The involvement of photosystem II-generated $H_2O_2$ in photoinhibition. – FEBS Lett. **286**: 209-213, 1991.

Butenko Y., Lin A., Naveh L. *et al*.: Differential roles of the thylakoid lumenal Deg protease homologs in chloroplast proteostasis. – Plant Physiol. **178**: 1065-1080, 2018.

Chassin Y., Kapri-Pardes E., Sinvany G. *et al.*: Expression and characterization of the thylakoid lumen protease DegP1 from *Arabidopsis*. – Plant Physiol. **130**: 857-864, 2002.

Chen K., Li H., Chen Y. *et al.*: *TaSCL14*, a novel wheat (*Triticum aestivum* L.) *GRAS* gene, regulates plant growth, photosynthesis, tolerance to photooxidative stress, and senescence. – J. Genet. Genomics **42**: 21-32, 2015.

Chen S., Han X., Fang J. *et al.*: *Sedum alfredii SaNramp6* metal transporter contributes to cadmium accumulation in transgenic *Arabidopsis thaliana*. – Sci. Rep.-UK **7**: 13318, 2017.

Choudhury N.K., Behera R.K.: Photoinhibition of photosynthesis: Role of carotenoids in photoprotection of chloroplast constituents. – Photosynthetica **39**: 481-488, 2001.

Clausen T., Southan C., Ehrmann M.: The HtrA family of proteases: implications for protein composition and cell fate. – Mol. Cell **10**: 443-455, 2002.

Couée I., Sulmon C., Gouesbet G., El Amrani A.: Involvement of soluble sugars in reactive oxygen species balance and responses to oxidative stress in plants. – J. Exp. Bot. **57**: 449-459, 2006.

Elstner E.F., Heupel A.: Inhibition of nitrite formation from hydroxylammoniumchloride: a simple assay for superoxide dismutase. – Anal. Biochem. **70**: 616-620, 1976.

Haußühl K., Andersson B., Adamska I.: A chloroplast DegP2 protease performs the primary cleavage of the photodamaged D1 protein in plant photosystem II. – EMBO J. **20**: 713-722, 2001.

Hein I., Barciszewska-Pacak M., Hrubikova K. *et al.*: Virus-induced gene silencing-based functional characterization of genes associated with powdery mildew resistance in barley. – Plant Physiol. **138**: 2155-2164, 2005.

Holzberg S., Brosio P., Gross C., Pogue G.P.: Barley stripe mosaic virus-induced gene silencing in a monocot plant. – Plant J. **30**: 315-327, 2002.

Horton P.: Prospects for crop improvement through the genetic manipulation of photosynthesis: morphological and biochemical aspects of light capture. – J. Exp. Bot. **51**: 475-485, 2000.

Huesgen P.F., Schuhmann H., Adamska I.: The family of Deg proteases in cyanobacteria and chloroplasts of higher plants. – Physiol. Plantarum **123**: 413-420, 2005.

Junglee S., Urban L., Sallanon H., Lopez-Lauri F.: Optimized assay for hydrogen peroxide determination in plant tissue using potassium iodide. – Am. J. Anal. Chem. **5**: 730-736, 2014.

Kapri-Pardes E., Naveh L., Adam Z.: The thylakoid lumen protease Deg1 is involved in the repair of photosystem II from photoinhibition in *Arabidopsis*. – Plant Cell **19**: 1039-1047, 2007.

Kato Y., Sun X., Zhang L., Sakamoto W.: Cooperative D1 degradation in the photosystem II repair mediated by chloroplastic proteases in *Arabidopsis*. – Plant Physiol. **159**: 1428-1439, 2012.

Ledwożyw A., Michalak J., Stepień A., Kądziołka A.: The relationship between plasma triglycerides, cholesterol, total lipids and lipid-peroxidation products during human atherosclerosis. – Clin. Chim. Acta **155**: 275-283, 1986.

Li H., Tong Y., Li B. *et al.*: Genetic analysis of tolerance to photo-oxidative stress induced by high light in winter wheat (*Triticum aestivum* L.). – J. Genet. Genomics **37**: 399-412, 2010.

Li H., Zheng Q., Zhang J. *et al.*: The analysis of determining factors and evaluation of tolerance to photoinhibition in wheat (*Triticum aestivum* L.). – Photosynthetica **55**: 69-76, 2017.

Li W.C., Liu Y.N., Liu M.M. *et al.*: Sugar accumulation is associated with leaf senescence induced by long-term high light in wheat. – Plant Sci. **287**: 110169, 2019.

Liu Y.N., Xu Q.Z., Li W.C. *et al.*: Long-term high light stress induces leaf senescence in wheat (*Triticum aestivum* L.). – Photosynthetica **57**: 830-840, 2019.

Luciński R., Misztal L., Samardakiewicz S., Jackowski G.: Involvement of Deg5 protease in wounding-related disposal of PsbF apoprotein. – Plant Physiol. Bioch. **49**: 311-320, 2011b.

Luciński R., Misztal L., Samardakiewicz S., Jackowski G.: The thylakoid protease Deg2 is involved in stress-related degradation of the photosystem II light-harvesting protein Lhcb6 in *Arabidopsis thaliana*. – New Phytol. **192**: 74-86, 2011a.

Miyao M.: Involvement of active oxygen species in degradation of the D1 protein under strong illumination in isolated subcomplexes of photosystem II. – Biochemistry **33**: 9722-9730, 1994.

Pan C., Lu H., Yu J. *et al.*: Identification of cadmium-responsive *Kandelia obovata* SOD family genes and response to Cd toxicity. – Environ. Exp. Bot. **162**: 230-238, 2019.

Peltier J.-B., Emanuelsson O., Kalume D.E. *et al.*: Central functions of the lumenal and peripheral thylakoid proteome of *Arabidopsis* determined by experimentation and genome-wide prediction. – Plant Cell **14**: 211-236, 2002.

Peskin A.V., Winterbourn C.C.: A microtiter plate assay for superoxide dismutase using a water-soluble tetrazolium salt (WST-1). – Clin. Chim. Acta **293**: 157-166, 2000.

Petty I.T.D., Hunter B.G., Wei N., Jackson A.O.: Infectious barley stripe mosaic virus RNA transcribed *in vitro* from full-length genomic cDNA clones. – Virology **171**: 342-349, 1989.

Pospíšil P., Yamamoto Y.: Damage to photosystem II by lipid peroxidation products. – BBA-Gen. Subjects **1861**: 457-466, 2017.

Schmittgen T.D., Livak K.J.: Analyzing real-time PCR data by the comparative $C_T$ method. – Nat. Protoc. **3**: 1101-1108, 2008.

Schubert M., Petersson U.A., Haas B.J. *et al.*: Proteome map of the chloroplast lumen of *Arabidopsis thaliana*. – J. Biol. Chem. **277**: 8354-8365, 2002.

Schuhmann H., Adamska I.: Deg proteases and their role in protein quality control and processing in different subcellular compartments of the plant cell. – Physiol. Plantarum **145**: 224-234, 2012.

Schuhmann H., Mogg U., Adamska I.: A new principle of oligomerization of plant DEG7 protease based on interactions of degenerated protease domains. – Biochem. J. **435**: 167-174, 2011.

Scofield S.R., Huang L., Brandt A.S., Gill B.S.: Development of a virus-induced gene-silencing system for hexaploid wheat and its use in functional analysis of the *Lr21*-mediated leaf rust resistance pathway. – Plant Physiol. **138**: 2165-2173, 2005.

Sima Y.-H., Yao J.-M., Hou Y.-S. *et al.*: Variations of hydrogen peroxide and catalase expression in Bombyx eggs during diapause initiation and termination. – Arch. Insect Biochem. Physiol. **77**: 72-80, 2011.

Sinvany-Villalobo G., Davydov O., Ben-Ari G. *et al.*: Expression in multigene families. Analysis of chloroplast and mitochondrial proteases. – Plant Physiol. **135**: 1336-1345, 2004.

Stevens R., Buret M., Garchery C. *et al.*: Technique for rapid, small-scale analysis of vitamin C levels in fruit and application to a tomato mutant collection. – J. Agr. Food Chem. **54**: 6159-6165, 2006.

Stirbet A., Lazár D., Kromdijk J., Govindjee: Chl *a* fluorescence

induction: Can just a one-second measurement be used to quantify abiotic stress responses? – Photosynthetica **56**: 86-104, 2018.

Su T., Wang P., Li H. *et al*.: The *Arabidopsis* catalase triple mutant reveals important roles of catalases and peroxisome-derived signaling in plant development. – J. Integr. Plant Biol. **60**: 591-607, 2018.

Sulmon C., Gouesbet G., Coueé I., El Amrani A.: Sugar induced tolerance to atrazine in *Arabidopsis* seedlings: interacting effects of atrazine and soluble sugars on *psbA* mRNA and D1 protein levels. – Plant Sci. **167**: 913-923, 2004.

Sun X.W., Fu T.J., Chen N. *et al*.: The stromal chloroplast Deg7 protease participates in the repair of photosystem II after photoinhibition in *Arabidopsis*. – Plant Physiol. **152**: 1263-1273, 2010.

Sun X.W., Peng L.W., Guo J.K. *et al*.: Formation of DEG5 and DEG8 complexes and their involvement in the degradation of photodamaged photosystem II reaction center D1 protein in *Arabidopsis*. – Plant Cell **19**: 1347-1361, 2007a.

Sun X.W., Wang L.Y., Zhang L.X.: Involvement of Deg5 and Deg8 proteases in the turnover of the photosystem II reaction center D1 protein under heat stress in *Arabidopsis thaliana*. – Chin. Sci. Bull. **52**: 1742-1745, 2007b.

Tikkanen M., Mekala N.R., Aro E.-M.: Photosystem II photoinhibition-repair cycle protects Photosystem I from irreversible damage. – BBA-Bioenergetics **1837**: 210-215, 2014.

Traverso N., Menini S., Maineri E.P. *et al*.: Malondialdehyde, a lipoperoxidation-derived aldehyde, can bring about secondary oxidative damage to proteins. – J. Gerontol. A **59**: B890-895, 2004.

Uauy C., Distelfeld A., Fahima T. *et al*.: A NAC gene regulating senescence improves grain protein, zinc, and iron content in wheat. – Science **314**: 1298-1301, 2006.

Ullah S., Kolo Z., Egbichi I. *et al.*: Nitric oxide influences glycine betaine content and ascorbate peroxidase activity in maize. – S. Afr. J. Bot. **105**: 218-225, 2016.

Wang L., Wang Y., Wang X. *et al.*: Regulation of POD activity by pelargonidin during vegetative growth in radish (*Raphanus sativus* L.). – Sci. Hortic.-Amsterdam **174**: 105-111, 2014.

Wu K., Li J., Luo J. *et al*.: Effects of elevated $CO_2$ and endophytic bacterium on photosynthetic characteristics and cadmium accumulation in *Sedum alfredii*. – Sci. Total Environ. **643**: 357-366, 2018.

Ying Y., Liu F.F., Li G.P. *et al*.: Silencing of the receptor-like cytoplasmic kinase gene *TaRKL1* reduces photosynthetic capacity in wheat. – Photosynthetica **58**: 1188-1199, 2020.

© The authors. This is an open access article distributed under the terms of the Creative Commons BY-NC-ND Licence.